ORGANIC CHEMISTRY FRONTIERS

CCS 中国化学会 CHINESE CHEMICAL SOCIETY

SIOC

ROYAL SOCIETY OF CHEMISTRY

Importance of Favourable Non-Covalent Contacts in the Stereoselective Synthesis of Tetrasubstituted Chromanone

Journal:	*Organic Chemistry Frontiers*
Manuscript ID	QO-RES-01-2022-000090.R1
Article Type:	Research Article
Date Submitted by the Author:	05-Apr-2022
Complete List of Authors:	Andreola, Laura; University of Georgia, Department of Chemistry Wheeler, Steven; University of Georgia, Department of Chemistry

ARTICLE

Importance of Favourable Non-Covalent Contacts in the Stereoselective Synthesis of Tetrasubstituted Chromanones

Received 00th January 20xx,
Accepted 00th January 20xx

DOI: 10.1039/x0xx00000x

Laura R. Andreola [a] and Steven E. Wheeler*[a]

Automated transiton state (TS) structure computations for a recently reported Pd-catalysed conjugated addition of arylboronic acids to 2-substituted chromones (*Chem Sci*, 2020, **11**, 4602) reveal unexpected conformations of the key stereodifferentiating benzyl group on the pyridine-dihydroisoquinoline (PyDHIQ) ligand. Detailed analysis shows that stereoselectivity is determined primarily by favourable non-covalent contacts between this benzyl group and the substrates, combined with torsional strain in the primary TS structure leading to the minor stereoisomer. This finding should inform further use and analysis of PyDHIQ and related ligands in other stereoselective transformations.

Introduction

Stoltz, Hong, and co-workers[1] recently developed new chiral pyridine-dihydroisoquinoline ligands (PyDHIQ, Scheme 1a) that enable the enantioselective synthesis of tetrasubstituted chromanones via a Pd-catalysed conjugate addition of arylboronic acids to 2-substituted chromones in aqueous solvent [Reaction (1), Scheme 1b]. Such chiral motifs are prevalent in natural products,[2-4] and this was the first demonstration of the enantioselective construction of a tetrasubstituted centre at the C_2 position of chromanones in a single step. Reaction (1) builds on previous examples of Pd(II) catalysed conjugate additions of arylboronic acids to α,β-unsaturated carbonyl groups from Uemura *et al.*,[5] Miyaura *et al.*,[6] and others.[7-15] In 2013, Stoltz et al.[16] accomplished the first Pd(II) catalysed conjugate addition of an arylboronic acid to chromone with moderate yields and high enantioselectivities with their *t*-BuPyOx ligand; however, they were only able to achieve trisubstituted stereocentres. In 2016, Gerten and Stanley[17] reported the racemic synthesis of tetrasubstituted chromanones via the addition of arylboronic acids to 2-substituted chromones in aqueous conditions with a $Pd(Phen)(TFA)_2$ catalyst. The 2020 report from Hong and coworkers[1] builds on these two previous results to achieve the enantioselective synthesis of tetrasubstituted chromanones in Scheme 1b.

Stoltz *et al.*[9] had previously reported the first enantioselective Pd-catalysed construction of all-carbon quaternary stereocentres via 1,4-addition of arylboronic acids to β-substituted cyclic enones. A subsequent computational study with Houk and co-workers[18] found that the mechanism involves transmetalation followed by coordination of the enone to the metal, alkene insertion, and protonation of the resulting enolate to yield the final product. These computations revealed that the alkene insertion step (see Scheme 1c) is both rate limiting and stereodetermining. Wiest *et al.*[19] recently used their Q2MM approach[20] to predict the stereoselectivity of 82 examples of this reaction based on this alkene insertion step, resulting in good agreement with experimental data. This further supports the alkene insertion step as the key to stereoselectivity.

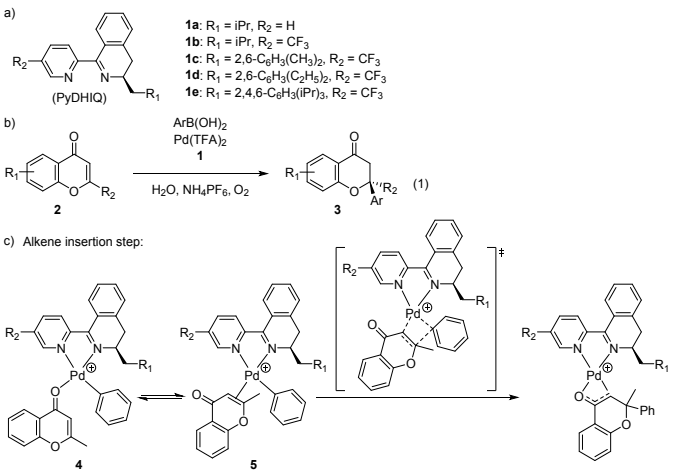

Scheme 1. (a) Chiral PyDHIQ ligands used by Hong and coworkers to catalyse (b) the enantioselective addition of arylboronic acids to 2-substitued chromones. (c) The stereodetermining alkene insertion step.

The selectivity of reaction (1) hinges on the identity of the stereodifferentiating group (R_1, Scheme 1a) on the chiral imine component of the PyDHIQ ligand.[1] Isopropyl groups at this position (e.g. ligand **1b**) lead to poor selectivity, while alkyl-substituted benzyl groups provide *ee*'s as high as 98%.

[a] *Department of Chemistry, University of Georgia, Athens, GA (USA). Email: swheele2@uga.edu*

Electronic Supplementary Information (ESI) available: [details of any supplementary information available should be included here]. See DOI: 10.1039/x0xx00000x

Furthermore, while bulkier alkyl groups (*i*Pr, *t*Bu) retain high selectivity they result in reduced yield. Ultimately, ligand **1c**, featuring a pendant 2,6-dimethylbenzyl group, was identified as the optimal catalyst for this reaction.

Hong and co-workers[1] explained the stereoselectivity of this transformation based on the TS model presented in Figure 1a. In this model, it was assumed that the chromone was located *cis* to the chiral imine component of the ligand in both the favoured and disfavoured TS. It was further assumed that the pendant benzyl group of the ligand was oriented away from the reaction centre based on an X-ray crystal structure of ligand **1d** bound to $PdCl_2$ that shows a similar conformation. The selectivity was then rationalized in terms of a proposed steric clash between the carbonyl group of the reacting chromone with the sterically-demanding R groups on the benzyl group.

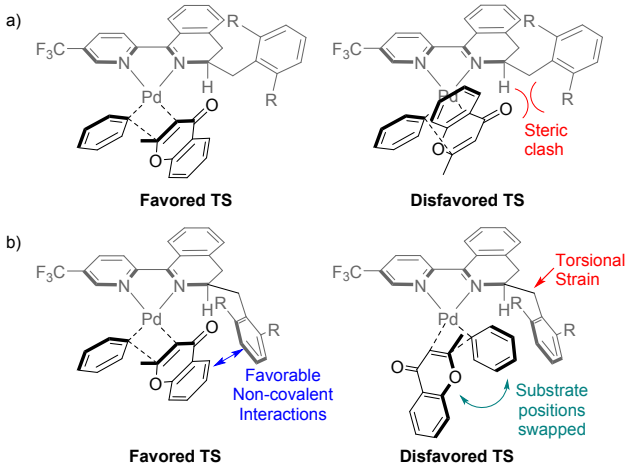

Figure 1. (a) TS model from Hong, *et al*.[1] (b) Revised TS model explaining the observed stereoselectivity in terms of stabilizing aryl-aryl interactions in the favoured TS complemented by torsional strain that destabilizes the disfavoured TS.

Herein, we provide a detailed computational study of reaction (1), showing that the coordination of the ligands to the Pd centre differs in the favoured and disfavoured pathways and in both stereocontrolling TS structures the benzyl group of PyDHIQ adopts a 'closed' conformation. This unexpected conformation proves vital for both the attractive non-covalent interactions that preferentially stabilize the TS structure leading to the major product and the torsional strain that disfavours the TS structure leading to the minor product (see Figure 1b).

Theoretical Methods

In light of previous mechanistic work,[18, 19] we focus on the rate-limiting and stereodetermining alkene insertion step for reaction (1) and further assume that the selectivity is under Curtin-Hammett control.[21] For ligand **1c**, we considered four primary options for these TS structures arising from the two possible configurations of the substrates (*i.e.* the chromone *cis* or *trans* to the chiral amine component of the ligand) and the addition to the two faces of the chromone. For each of these structures, conformations were systematically explored using Crest[22] (constraining positions of the bond-forming atoms) at the GFN2-xTB level of theory,[23] retaining all unique conformers (based on a 0.125 Å RMSD cut-off) within 10 kcal mol^{-1} of the lowest-lying conformer. These structures were then fully optimized at the B3LYP-D3/6-31G(d)/LANL2DZ[24-27] level of theory common to other DFT studies involving Pd,[28] using PCM[29, 30] to model the aqueous solvent. All TS structures were confirmed to have a single imaginary vibrational frequency with mode corresponding to the forming C–C bond. In total, 35 unique TS structures were identified for **1c** based on an RMSD cut-off of 0.4 Å. Single point energies were then computed at the PCM-B3LYP-D3BJ/6-311+G(d,p)/LANL2DZ[31] level of theory. After these structures were identified for **1c**, the lowest energy structures leading to the (*R*) and (*S*) products were used as template structures for the automated TS optimizer AARON[32] to find analogous TS structures for ligands **1a**, **1b**, **1d**, and **1e**. AARON automatically samples conformations of added substituents.

The reported free energies comprise the PCM-B3LYP-D3BJ/6-311+G(d,p)/LANL2DZ single point energies with thermal and entropic corrections calculated using Grimme's quasi-RRHO approximation[33] from frequencies computed at 333 K at the PCM-B3LYP-D3/6-31G(d)/LANL2DZ level of theory, which are then Boltzmann weighted. All DFT computations were executed with Gaussian 09,[34] with input generation, output parsing, and thermochemical analysis done using AaronTools.[35] Molecular structure figures and the buried volume visualization in the TOC figure were generated using UCSF ChimeraX[36] with the SEQCROW bundle.[35, 37]

Results and Discussion

A. Ligand Conformations

The key benzyl group in ligands **1c**, **1d**, and **1e** can adopt either an 'open' or 'closed' conformation (see Figure 2). The X-ray crystal structure of **1d** (featuring a 2,6-diethylbenzyl substituent) bound to $PdCl_2$, reported by Hong *et al*.,[1] reveals that the Bn group is oriented away from the Pd. Gas phase DFT computations of the analogous complex featuring ligand **1c** predict that the open and closed conformer are nearly isoergonic, with the latter lying only 0.4 kcal mol^{-1} lower in free energy than the former. In aqueous solvent the free energy gap increases, with the closed conformer predicted to be 1.4 kcal mol^{-1} lower in free energy than the open conformer (see Figure 2). Interestingly, the unbound ligand favours the open conformation found in the X-ray crystal structure, but only slightly, by 0.7 kcal mol^{-1} in the gas phase and 0.1 kcal mol^{-1} in aqueous solvent (see ESI Table S5). This suggests the importance of the interaction of the benzyl group with some combination of the palladium and the chlorines in the conformational behaviour of this ligand, which portends the important role that the benzyl group conformation plays in the energetics of the catalytically active complex.

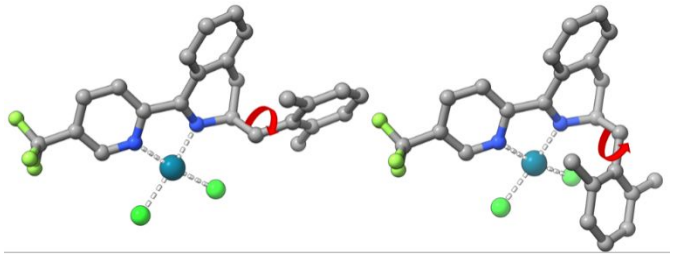

	ΔG (open)	ΔG (closed)
Gas phase	0.4	0.0
Solvent	1.4	0.0

Figure 2. Optimized structures of the 'open' and 'closed' conformations of **1c**-$PdCl_2$ along with relative free energies in the gas phase and in solution provided in kcal mol^{-1}. Hydrogens omitted for clarity.

B. Stereocontrolling TS Structures and Origin of Stereoselectivity

The key alkene insertion step in reaction (1) is depicted in Scheme 1c. Stereoselectivities were predicted for five ligands (see Table 1) based on an exhaustive search of possible conformations and configurations of the ligands around the metal centre (see Theoretical Methods, above, and Supplementary Information). Overall, there is reasonable agreement between the computed and experimental selectivities, although we systematically overestimate the free energy difference between the stereocontrolling TS structures. However, we correctly capture the key experimental observation that bulky aryl groups are required for high selectivity. Although ligand **1a** was not experimentally active, we predict that, if catalytically active, its selectivity would follow this trend.

Table 1. Experimental yield, *ee*, and free energy barrier differences ($\Delta\Delta G^{\ddagger}$) along with predicted barrier height ($\Delta G^{\ddagger}$), *ee*, and $\Delta\Delta G^{\ddagger}$ values (in kcal mol^{-1}) for reaction (1) using different PyDHIQ ligands.

	Experiment			Theory		
Ligand	% Yield	*ee*	$\Delta\Delta G^{\ddagger}$	$\Delta G^{\ddagger}$	*ee*	$\Delta\Delta G^{\ddagger}$
1a	-	-	-	21.8	92	2.1
1b	11	68	1.1	20.3	98	3.0
1c	97	95	2.4	20.5	>99	4.8
1d	77	98	3.0	20.1	>99	5.0
1e	70	98	3.0	18.9	>99	7.3

To explain the origin of the selectivity in this reaction, we examined the key low-lying TS structures leading to the two stereoisomeric products for ligand **1c** more closely (see Figure 3). Notably, in the most favourable TS structures the substituted benzyl group of the ligand adopts the closed conformation in which it is rotated toward the Pd and reacting substrates. This is in contrast with the conformer assumed by Hong *et al*.[1]

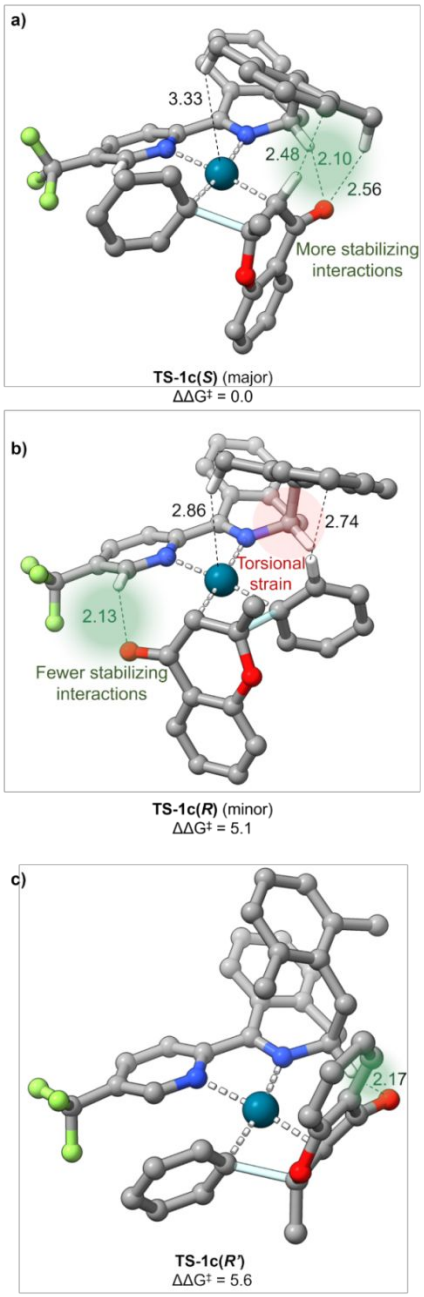

Figure 3. Optimized structures a) and b) of the stereocontrolling TS structures and c) of the pro-R TS structure with the chromone cis to R_2 for reaction 1 catalysed by **1c.** Key distances are shown in Angstroms and relative free energies in kcal mol^{-1}. Selected hydrogens omitted for clarity. The stereocontrolling TS structure for ligands **1d** and **1e** are similar to those shown above. For ligands **1a** and **1b** the chromone is cis to R_2 in both pro-R and pro-S TS structures.

Moreover, while in **TS-1c(S)**, which leads to the major stereoisomer, the substrates adopt the configuration assumed by Hong *et al*.,[1] in the minor TS structure [**TS-1c(R)**] the chromone is *trans* to the chiral amine component of the ligand (Figure 3a). The lowest-lying TS(R) structure featuring the chromone *cis* to the chiral amine component of the ligand, **TS-1c(R')** (Figure 3c), is 0.5 kcal mol^{-1} higher in free energy than **TS-1c(R)**. Moreover, unlike the TS structures in Figures 3a and b, in this more highly disfavoured TS structure the Bn group adopts a conformation almost parallel to the aromatic portion of the

ligand. Thus, the steric interactions between the chromone and benzyl group envisioned by Hong *et al*.[1] (see Figure 1) are not present in the corresponding TS structure, which is furthermore not the primary TS structure leading to the minor stereoisomer!

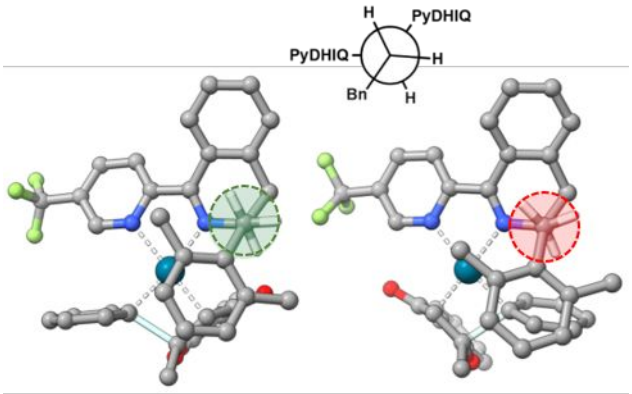

TS-**1c**(*S*) TS-**1c**(*R*)

Ligand	TS(S)	TS(R)	Bound to $PdCl_2$
1a	173.6	173.1	178.6
1b	169.3	173.0	178.9
1c	172.8	155.6	179.3
1d	175.1	156.4	176.5
1e	175.8	155.7	177.7

Figure 4. Optimized structures of the stereocontrolling TS structures for the reaction in Scheme 1 using **1c** with the benzyl-ligand dihedral angle highlighted. The key dihedral angle (in degrees, see Newman projection) is provided for the stereocontrolling TS structures for all four ligands. Selected hydrogens omitted for clarity.

Qualitatively, **TS-1c(S)** is favoured over **TS-1c(R)** due primarily to the presence of a greater number of stabilizing non-covalent interactions between the substrate and ligand in the former and destabilizing torsional strain of the Bn group in the latter. More precisely, it can be seen in Figures 3a and b that **TS-1c(S)** involves two stabilizing non-covalent interactions between the ketone oxygen of the chromone and two nearby hydrogens, while in **TS-1c(R)** only one such interaction is present. **TS-1c(R)** also has fewer stabilizing interactions between the benzyl group and the substrates than **TS-1c(S)** and these interactions are less favourable, with longer distances and less ideal interaction angles. Specifically, **TS-1c(S)** has three CH-π interactions between the substrate and the benzyl group ranging from 2.48 - 2.78 Å whereas **TS-1c(R)** has only one interaction at 2.78 Å. In terms of torsional strain, Figure 4 shows that the dihedral angle of the benzyl group relative to the ligand backbone is much closer to the preferred angle (*i.e.* that of the ligand bound to PdCl2; see Figure 4) in **TS-1c(S)** than in **TS-1c(R)** (172.8° vs 155.6°). In the latter case, this non-ideal dihedral angle arises to relieve a steric clash between the benzyl group and the benzene substrate. Finally, we note that one of the hydrogens on the aromatic ring of the Bn group engages in a weak agostic interaction with the Pd (see Figures 3a and b). This interaction is stronger in TS-1c(R) than in TS-1c(S) (e.g. the H···Pd distance is 2.86 Å in TS-1c(R) but 3.33 Å in TS-1c(S); see ESI Table S6 and Figure S2 for NBO analysis), resulting in a slight decrease in selectivity.

To quantify the non-covalent interactions between the ligand and substrate, we considered two complementary energy decomposition analyses (see Figure 5 and ESI for details). These consistently show that the non-covalent interactions between the ligand and substrate are 1.8 to 2.2 kcal/mol more favourable in **TS-1c(S)** compared to **TS-1c(R)**. Further decomposition of the ligand-substrate interaction indicates that the bulk of this difference (1.3 kcal/mol) can be attributed to the dimethyl benzyl group. In terms of the torsional strain of the benzyl groups in **TS-1c(S)** and **TS-1c(R)**, the distortion energy of the ligand is 1.2 kcal/mol greater in the latter than in the former (see Supporting Information for details).

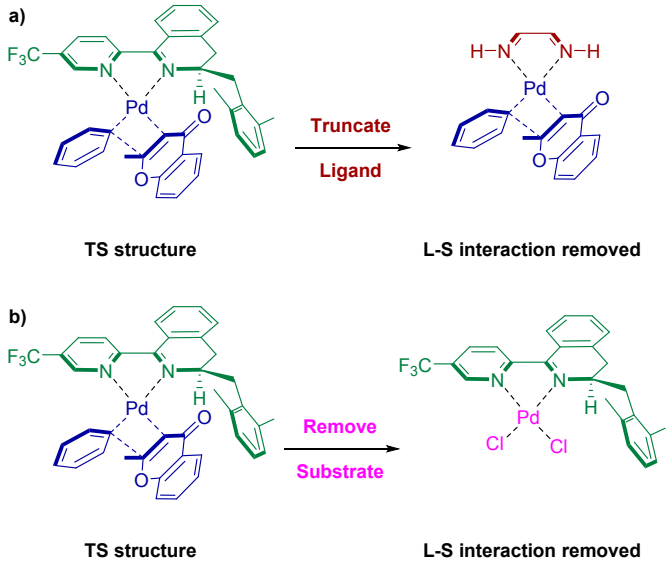

Figure 5. Models of the system without the Ligand-Substrate interaction where the ligand is truncated (a) and the substrate is removed (b).

Analyses of the key TS structures for ligands **1b**, **1d**, and **1e** provide a more complete picture of the origins of stereoselectivity. First, unlike in the TS structures for ligands with bulky R_1 groups, for ligand **1b** both low-lying TS structures feature the chromone *trans* to the chiral amine component of the ligand. The modest selectivity of this ligand originates from the more favourable hydrogen bonding interaction formed between the chromone and ligand in the TS structure leading to the (S) product [in TS-1b(S) this interaction has a distance of 2.05 Å and an angle of 148.4°, compared to 2.09 Å and 132.0°in TS-1b(R)].

The introduction of a bulky substituent (i.e. ligands **1c**, **1d**, and **1e**) drastically destabilizes the (R)-transition state featuring the chromone *trans* to chiral amine due to the distortion of the ligand required to avoid a steric clash. The result for all three of these ligands is that the operative TS structure leading to the (R) stereoisomer features the chromone *cis* to the chiral amine, as seen for ligand **1c** in Figure 3b. However, ligand distortion is not completely avoided in these *cis* structures, all of which exhibit

non-ideal dihedral angles (see Figure 4). For all three ligands the dihedral angle is ~20° farther from ideal in TS(R) than in TS(S). Thus, the origins of stereoselectivity of ligands **1d** and **1e** are similar to those discussed for **1c** and arise from a combination of the more favourable non-covalent contacts between the ligand and substrate in the (S)-transition state structures combined with the torsional strain in the ligand in the TS structures leading to the (R) product. This is depicted in the revised stereoselectivity model in Figure 1b.

C. Intermediates 4 and 5

To further understand this reaction, we also considered intermediates **4** and **5**. Based on previous work,[18] catalytic activity is expected to be primarily determined by the free energy difference between the lowest-lying TS structure and the intermediate **4** ($\Delta G^{\ddagger}$, see Table 1). While the experimental yields cannot be fully explained by these predicted barrier heights alone, the computed values do correctly predict ligand **1a** to be considerably less active than the other ligands.

In terms of intermediate **5**, which immediately precedes **TS-1c(S)** and **TS-1c(R)** (see Figure 6) in the catalytic cycle, we again find that the closed conformations are lower in free energies than their open counterparts. The difference between the open and closed energies is slightly larger for intermediate **5-(S)**, suggesting that the interaction of the benzyl group with the substrates is more favourable in intermediate **5-(S)** than in **5-(R)** since it has a more stabilizing effect on the energy. This free energy difference can be explained, however, in relation to the stabilizing interactions and torsional angle of the ligands in the transition states. In **5-(S)-closed**, the key stabilizing interactions seen in **TS-1c-S** are not formed as favourably; the interaction between a benzyl hydrogen and the chromone carbonyl, at 2.56 Å in the transition state, has a 2.98 Å distance in **5-(S)**. Additionally, the destabilizing torsional strain in **TS-1c-R** is not observed in **5-(R)-closed**; the ligand does not have to accommodate the substrate phenyl which is not close enough to the chromone for bond formation. Both ligands have favourable benzyl dihedral angles in intermediate **5**.

Conclusions

Understanding the origin of stereoselectivity in catalytic reactions is instrumental in the rational design of improved chiral ligands. Above, we showed that the PyDHIQ ligand affords the stereoselective synthesis of tetrasubstituted chromanones primarily by engaging in stabilizing non-covalent interactions with the reacting chromone in the TS structure leading to the favoured enantiomer. These interactions include hydrogen bonding and dispersion-driven interactions, both of which are significant contributors to the difference in free energy barriers between the stereocontrolling TS structures. Dispersion forces are especially important in the interaction of the ligand with the chromone in the TS structure leading to the major stereoisomer, where the seemingly bulky benzyl group contributes favourably to the energy with stabilizing dispersion effects more than it does unfavourably with steric effects.[38] Because these interactions are localized on the end of the chromone where the reaction occurs, extending the use of this reaction scheme to other substrates with more complex scaffolds would potentially allow highly stereoselective preparation of more complex products with chromone motifs, which are significant in antibiotic and anticancer drug development.

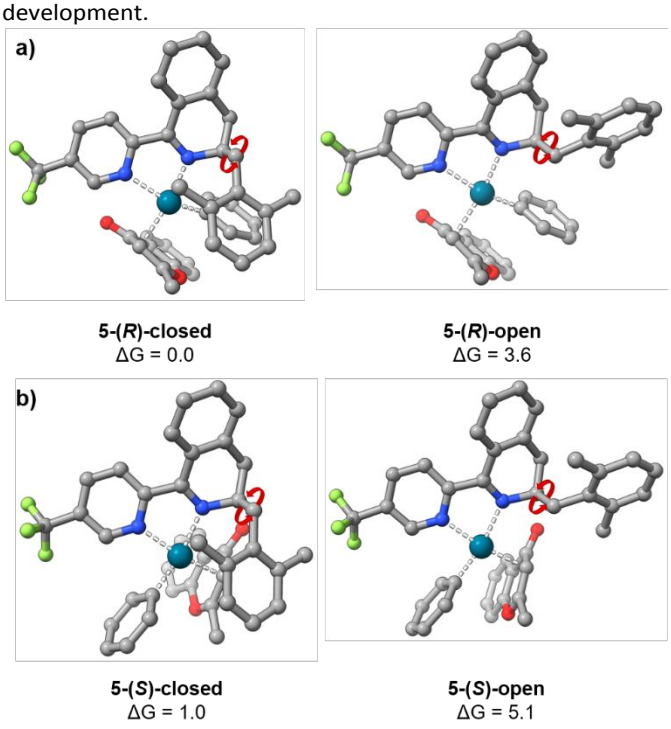

Figure 6. Optimized structures of intermediate **5** leading to **TS-1c(R)** (a) and **TS-1c(S)** (b) for ligand **1c** in open and closed ligand conformations. Free energies are relative to **5-(*R*)-closed** and given in kcal mol^{-1}.

More broadly, the 'closed' conformation of the PyDHIQ ligand favoured in the stereocontrolling TS structures for this reaction will likely also be operative in other reactions utilizing these ligands. Thus, even though the crystal structure of PyDHIQ bound to $PdCl_2$ exhibits an open conformation, one must consider both closed and open conformations of this ligand when developing stereochemical models of reactions in which it is utilized. For example, Hong *et al*.[39] recently reported another use of PyDHIQ ligand **1c** in an Ir catalysed C(sp^2)-H borylation of diarylmethylsilanes. Due to the bulkiness of the Bpin group in the substrate and the possibility of both stabilizing and destabilizing interactions between the Bpin and benzyl groups of the ligand, it would be necessary to explore the 'closed' and 'open' conformers of the ligand to determine the factors responsible for this high degree of selectivity.

Author Contributions

LRA is responsible for the data curation, formal analysis, visualization, and writing of the original draft; SEW is responsible for conceptualization and review and editing of the manuscript.

Conflicts of interest

There are no conflicts to declare.

Acknowledgements

This work was supported by National Science Foundation Grant CHE-1665407 and conducted using high performance computing resources provided by the Georgia Advanced Computing Resource Center (http://gacrc.uga.edu).

Notes and references

1. D. Baek, H. Ryu, J. Y. Ryu, J. Lee, B. M. Stoltz and S. Hong, Catalytic enantioselective synthesis of tetrasubstituted chromanones via palladium-catalyzed asymmetric conjugate arylation using chiral pyridine-dihydroisoquinoline ligands. *Chem Sci*, 2020, **11**, 4602-4607.
2. S. Emami and Z. Ghanbarimasir, Recent advances of chroman-4-one derivatives: Synthetic approaches and bioactivities. *European Journal of Medicinal Chemistry*, 2015, **93**, 539-563.
3. F. E. Ward, D. L. Garling, R. T. Buckler, D. M. Lawler and D. P. Cummings, Antimicrobial 3-methylene flavanones. *Journal of Medicinal Chemistry*, 1981, **24**, 1073-1077.
4. A. Gaspar, M. J. Matos, J. Garrido, E. Uriarte and F. Borges, Chromone: A Valid Scaffold in Medicinal Chemistry. *Chemical Reviews*, 2014, **114**, 4960-4992.
5. C. S. Cho, S.-i. Motofusa, K. Ohe and S. Uemura, Palladium(II)-catalyzed conjugate addition of aromatics to α,β-unsaturated ketones and aldehydes with arylantimony compounds. *Bull. Chem. Soc. Jpn.*, 1996, **69**, 2341-2348.
6. T. Nishikata, Y. Yamamoto and N. Miyaura, Conjugate addition of aryl boronic acids to enones catalyzed by cationic palladium(II)-phosphane complexes. *Angew. Chem., Int. Ed.*, 2003, **42**, 2768-2770.
7. R. B. Bedford, M. Betham, J. P. H. Charmant, M. F. Haddow, A. G. Orpen, L. T. Pilarski, S. J. Coles and M. B. Hursthouse, Simple Palladacyclic and Platinacyclic Catalysts for the 1,4-Conjugate Addition of Arylboronic Acids and Arylsiloxanes to Enones. *Organometallics*, 2007, **26**, 6346-6353.
8. P. He, Y. Lu, C.-G. Dong and Q.-S. Hu, Anionic Four-Electron Donor-Based Palladacycles as Catalysts for Addition Reactions of Arylboronic Acids with α,β-Unsaturated Ketones, Aldehydes, and α-Ketoesters. *Org. Lett.*, 2007, **9**, 343-346.
9. K. Kikushima, J. C. Holder, M. Gatti and B. M. Stoltz, Palladium-catalyzed asymmetric conjugate addition of arylboronic acids to five-, six-, and seven-membered β-substituted cyclic enones: enantioselective construction of all-carbon quaternary stereocenters. *J. Am. Chem. Soc.*, 2011, **133**, 6902-6905.
10. S. Lin and X. Lu, Cationic Pd(II)/bipyridine-catalyzed conjugate addition of arylboronic acids to β,β-disubstituted enones: construction of quaternary carbon centers. *Org. Lett.*, 2010, **12**, 2536-2539.
11. X. Lu and S. Lin, Pd(II)-Bipyridine Catalyzed Conjugate Addition of Arylboronic Acid to α,β-Unsaturated Carbonyl Compounds. *J. Org. Chem.*, 2005, **70**, 9651-9653.
12. T. Nishikata, Y. Yamamoto and N. Miyaura, 1,4-Addition of Arylboronic Acids and Arylsiloxanes to α,β-Unsaturated Carbonyl Compounds via Transmetalation to Dicationic Palladium(II) Complexes. *Organometallics*, 2004, **23**, 4317-4324.
13. T. Nishikata, Y. Yamamoto and N. Miyaura, Asymmetric 1,4-addition of arylboronic acids to α,β-unsaturated N-acylamides catalyzed by dicationic palladium(II)-(S,S)-chiraphos complex. *Chem. Lett.*, 2007, **36**, 1442-1443.
14. T. Nishikata, Y. Yamamoto and N. Miyaura, Palladium(II)-catalyzed 1,4-addition of arylboronic acids to β-arylenones for enantioselective synthesis of 4-aryl-4H-chromenes. *Adv. Synth. Catal.*, 2007, **349**, 1759-1764.
15. T. Nishikata, Y. Yamamoto and N. Miyaura, Palladium(II)-catalyzed 1,4-addition of arylboronic acids to β-arylenals for enantioselective syntheses of 3,3-diarylalkanals: a short synthesis of (+)-(R)-CDP 840. *Tetrahedron Lett.*, 2007, **48**, 4007-4010.
16. J. C. Holder, A. N. Marziale, M. Gatti, B. Mao and B. M. Stoltz, Palladium-catalyzed asymmetric conjugate addition of arylboronic acids to heterocyclic acceptors. *Chem. - Eur. J.*, 2013, **19**, 74-77.
17. A. L. Gerten and L. M. Stanley, Palladium-catalyzed conjugate addition of arylboronic acids to 2-substituted chromones in aqueous media. *Tetrahedron Letters*, 2016, **57**, 5460-5463.
18. J. C. Holder, L. Zou, A. N. Marziale, P. Liu, Y. Lan, M. Gatti, K. Kikushima, K. N. Houk and B. M. Stoltz, Mechanism and enantioselectivity in palladium-catalyzed conjugate addition of arylboronic acids to beta-substituted cyclic enones: insights from computation and experiment. *J Am Chem Soc*, 2013, **135**, 14996-15007.
19. J. Wahlers, M. Maloney, F. Salahi, A. R. Rosales, P. Helquist, P. O. Norrby and O. Wiest, Stereoselectivity Predictions for the Pd-Catalyzed 1,4-Conjugate Addition Using Quantum-Guided Molecular Mechanics. *J Org Chem*, 2021, **86**, 5660-5667.
20. A. R. Rosales, T. R. Quinn, J. Wahlers, A. Tomberg, X. Zhang, P. Helquist, O. Wiest and P. O. Norrby, Application of Q2MM to predictions in stereoselective synthesis. *Chem Commun (Camb)*, 2018, **54**, 8294-8311.
21. J. I. Seeman, Effect of conformational change on reactivity in organic chemistry. Evaluations, applications, and extensions of Curtin-Hammett Winstein-Holness kinetics. *Chemical Reviews*, 1983, **83**, 83-134.
22. P. Pracht, F. Bohle and S. Grimme, Automated exploration of the low-energy chemical space with fast quantum chemical methods. *Phys Chem Chem Phys*, 2020, **22**, 7169-7192.
23. C. Bannwarth, S. Ehlert and S. Grimme, GFN2-xTB—An Accurate and Broadly Parametrized Self-Consistent Tight-Binding Quantum Chemical Method with Multipole Electrostatics and Density-Dependent Dispersion Contributions. *Journal of Chemical Theory and Computation*, 2019, **15**, 1652-1671.
24. A. D. Becke, Density-functional thermochemistry. III. The role of exact exchange. *The Journal of Chemical Physics*, 1993, **98**, 5648-5652.

25. S. Grimme, J. Antony, S. Ehrlich and H. Krieg, A consistent and accurate ab initio parametrization of density functional dispersion correction (DFT-D) for the 94 elements H-Pu. *J Chem Phys*, 2010, **132**, 154104.
26. W. J. Hehre, R. F. Stewart and J. A. Pople, Self-Consistent Molecular-Orbital Methods. I. Use of Gaussian Expansions of Slater-Type Atomic Orbitals. *The Journal of Chemical Physics*, 1969, **51**, 2657-2664.
27. P. J. Hay and W. R. Wadt, Ab initio effective core potentials for molecular calculations. Potentials for the transition metal atoms Sc to Hg. *The Journal of Chemical Physics*, 1985, **82**, 270-283.
28. T. Sperger, I. A. Sanhueza, I. Kalvet and F. Schoenebeck, Computational Studies of Synthetically Relevant Homogeneous Organometallic Catalysis Involving Ni, Pd, Ir, and Rh: An Overview of Commonly Employed DFT Methods and Mechanistic Insights. *Chem Rev*, 2015, **115**, 9532-9586.
29. S. Miertus, E. Scrocco and J. Tomasi, Electrostatic Interaction of a Solute with a Continuum - a Direct Utilization of Abinitio Molecular Potentials for the Prevision of Solvent Effects. *Chem Phys*, 1981, **55**, 117-129.
30. J. Tomasi, B. Mennucci and R. Cammi, Quantum mechanical continuum solvation models. *Chem Rev*, 2005, **105**, 2999-3093.
31. S. Grimme, S. Ehrlich and L. Goerigk, Effect of the damping function in dispersion corrected density functional theory. *J Comput Chem*, 2011, **32**, 1456-1465.
32. Y. Guan, V. M. Ingman, B. J. Rooks and S. E. Wheeler, AARON: An Automated Reaction Optimizer for New Catalysts. *J Chem Theory Comput*, 2018, **14**, 5249-5261.
33. S. Grimme, Supramolecular binding thermodynamics by dispersion-corrected density functional theory. *Chemistry A European Journal*, 2012, **18**, 9955-9964.
34. M. Frisch, G. Trucks, H. Schlegel, G. Scuseria, M. Robb, J. Cheeseman, G. Scalmani, V. Barone, B. Mennucci, G. Petersson, H. Nakatsuji, M. Caricato, X. Li, H. Hratchian, A. Izmaylov, J. Bloino, G. Zheng, J. Sonnenberg, M. Hada, M. Ehara, K. Toyota, R. Fukuda, J. Hasegawa, M. Ishida, T. Nakajima, Y. Honda, O. Kitao, H. Nakai, T. Vreven, J. Montgomery, JA, J. Peralta, F. Ogliaro, M. Bearpark, J. Heyd, E. Brothers, K. Kudin, V. Staroverov, T. Keith, R. Kobayashi, J. Normand, K. Raghavachari, A. Rendell, J. Burant, S. Iyengar, J. Tomasi, M. Cossi, N. Rega, J. Millam, M. Klene, J. Knox, J. Cross, V. Bakken, C. Adamo, J. ramillo, R. Gomperts, R. Stratmann, O. Yazyev, A. Austin, R. Cammi, C. Pomelli, J. Ochterski, R. Martin, K. Morokuma, V. Zakrzewski, G. Voth, P. Salvador, J. Dannenberg, S. Dapprich, A. Daniels, O. Farkas, J. Foresman, J. Ortiz, J. Cioslowski and D. Fox, *Journal*, 2009.
35. V. M. Ingman, A. J. Schaefer, L. R. Andreola and S. E. Wheeler, QChASM: Quantum chemistry automation and structure manipulation. *WIREs Computational Molecular Science*, 2020, **11**, e1510.
36. E. F. Pettersen, T. D. Goddard, C. C. Huang, E. C. Meng, G. S. Couch, T. I. Croll, J. H. Morris and T. E. Ferrin, UCSF ChimeraX: Structure visualization for researchers, educators, and developers. *Protein Sci*, 2020, DOI: 10.1002/pro.3943.
37. A. J. Schaefer, V. M. Ingman and S. E. Wheeler, SEQCROW: A ChimeraX bundle to facilitate quantum chemical applications to complex molecular systems. *J Comput Chem*, 2021, **42**, 1750-1754.
38. J. P. Wagner and P. R. Schreiner, London dispersion in molecular chemistry--reconsidering steric effects. *Angew Chem Int Ed*, 2015, **54**, 12274-12296.
39. D. Park, D. Baek, C.-W. Lee, H. Ryu, S. Park, W. Han and S. Hong, Enantioselective C(sp2)–H borylation of diarylmethylsilanes catalyzed by chiral pyridine-dihydroisoquinoline iridium complexes. *Tetrahedron*, 2021, **79**, 131811.